

Gallic acid-assisted synthesis of nitrogen self-doped carbon microspheres for superb oxygen reduction and superior volumetric lithium storage

The computer controlled Neware battery tester was used for the galvanostatic charge-discharge of test cells. So we need to use the equations (5) and (6) in text to work out the volumetric capacity. The SEM crosssection of prepared NCM electrodes can be seen in Figure S1. The thickness (t) of electrode tested is ca.5.8 μm in our experiment.

The density of the electrode, ρ , can be calculated from the according equation ρ (g cm^{-3})= M (mg cm^{-2})/ t (cm), i.e., $\rho=M/t=0.706*10^{-3}/(5.8*10^{-4})/(\pi/4)=1.55$ (g cm^{-3}). So, at 0.1 A g^{-1} , $C_v=885.8$ $\text{mAh g}^{-1}*1.55$ $\text{g cm}^{-3}=1373$ mAh cm^{-3} ; at 1.0 A g^{-1} , $C_v=709.6*1.55=1100$ mAh cm^{-3} .

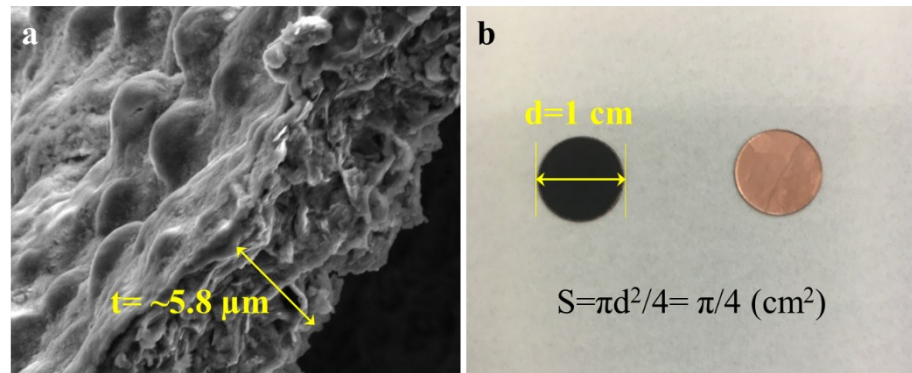


Figure S1. The prepared NCM electrodes. (a) SEM crosssection. (b) Optical photograph.

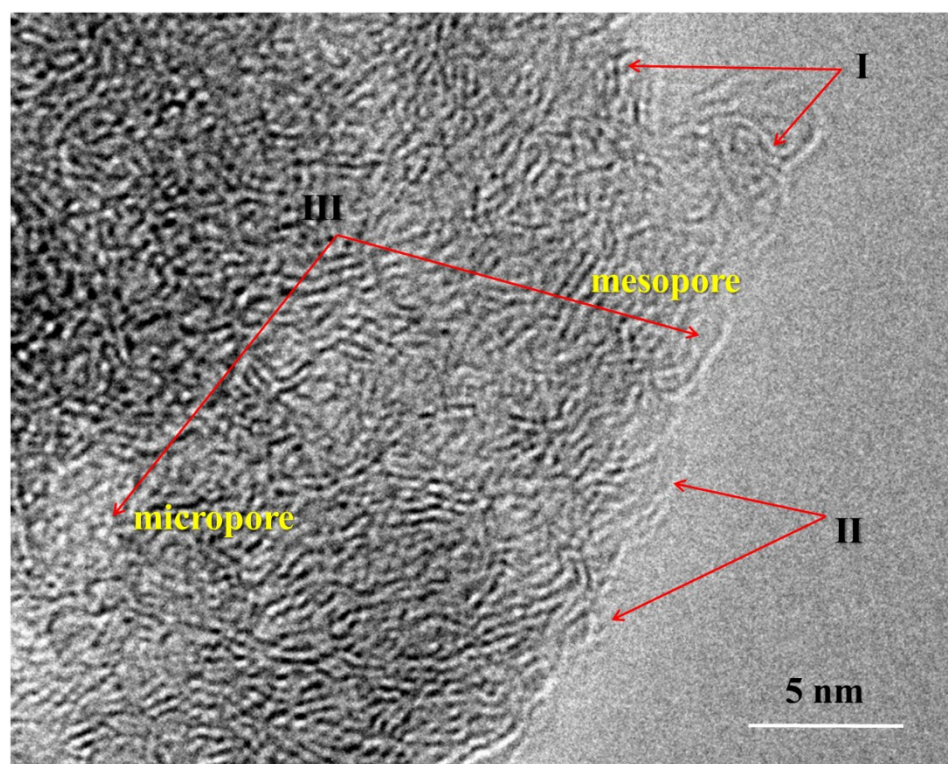


Figure S2. Schematic structural characters of the NCM. I, II, and III in panels represent three typical defective locations, i.e., the corner (I), the broken fringe (II), and the pore (III), respectively.

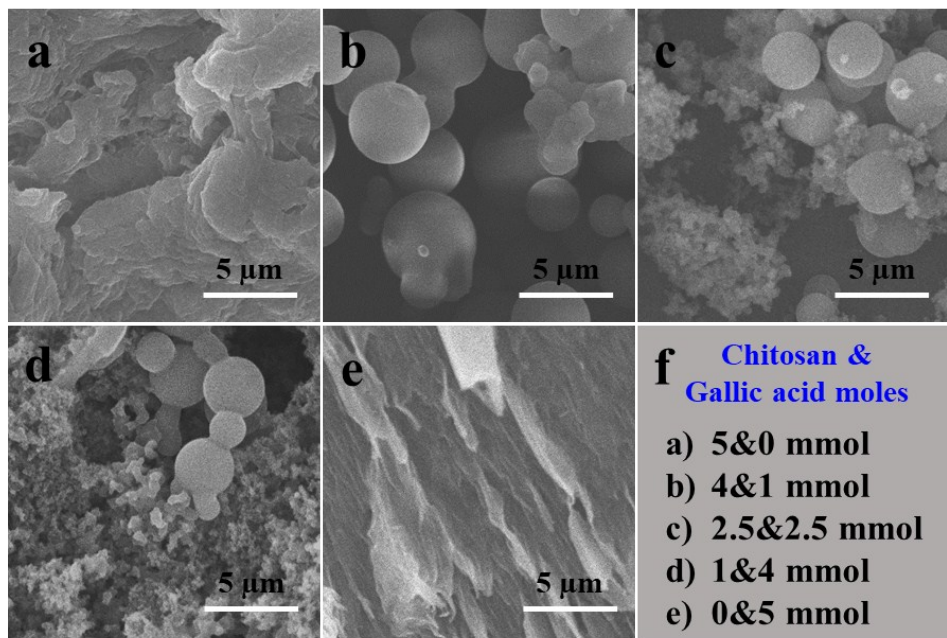


Figure S3. SEM images of different moles of chitosan and gallic acid, (a) 5&0 mmol, (b) 4&1 mmol, (c) 2.5&2.5 mmol, (d) 1&4 mmol, (e) 0&5 mmol.

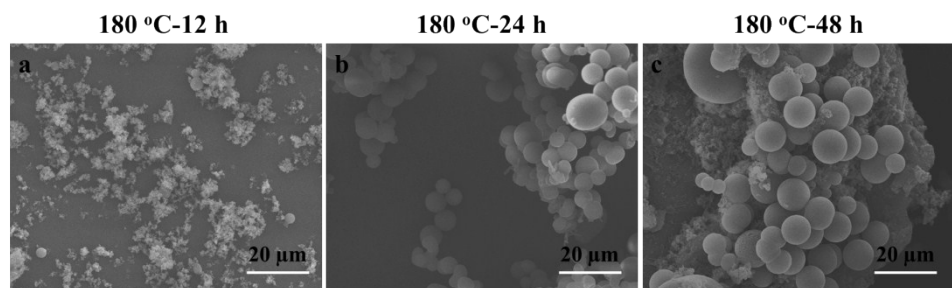


Figure S4. SEM images of the 4 mmol chitosan and 1 mmol gallic acid mixture treated at 180 °C for 12, 24 and 48 h, respectively.

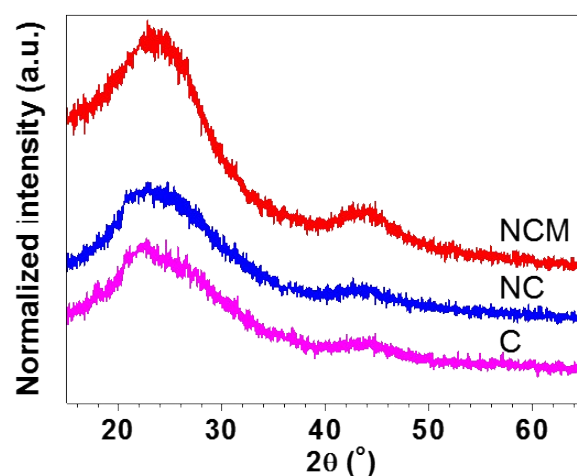


Figure S5. XRD patterns of NCM, NC, and C.

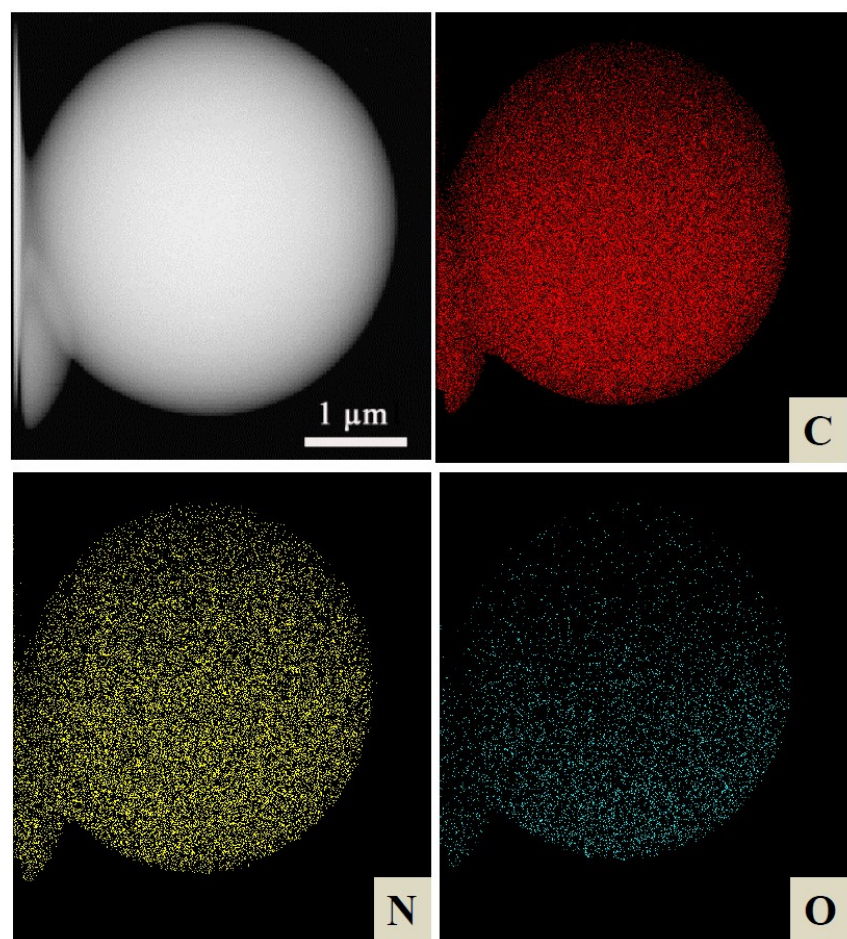


Figure S6. STEM image and corresponding elemental mappings for a single microsphere of NCM.

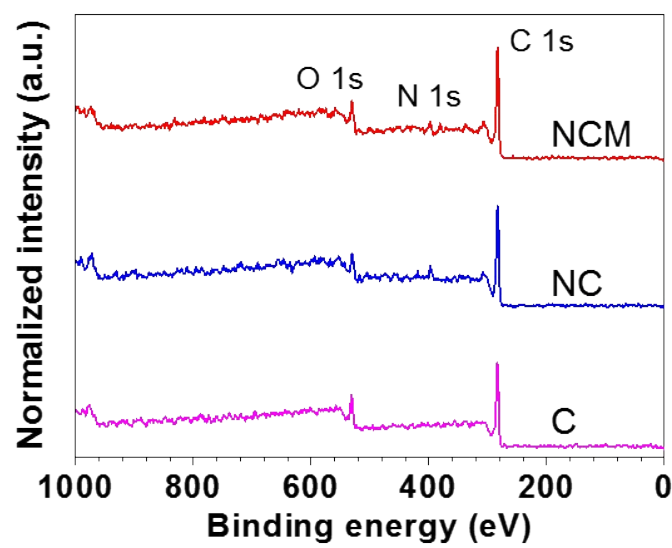


Figure S7. Survey XPS spectra for NCM, NC, and C.

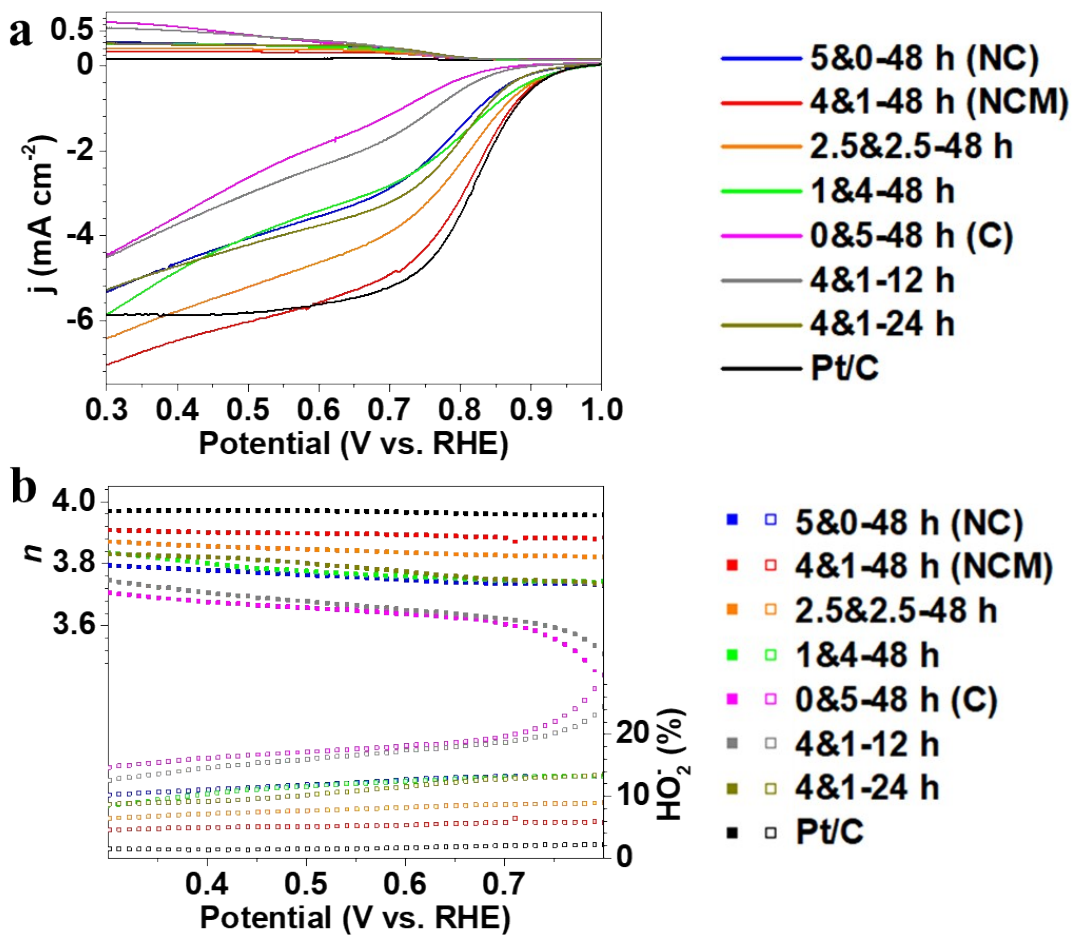


Figure S8. ORR performances of all samples. (a) LSV curves. (b) The corresponding plots of n and HO_2 yield.

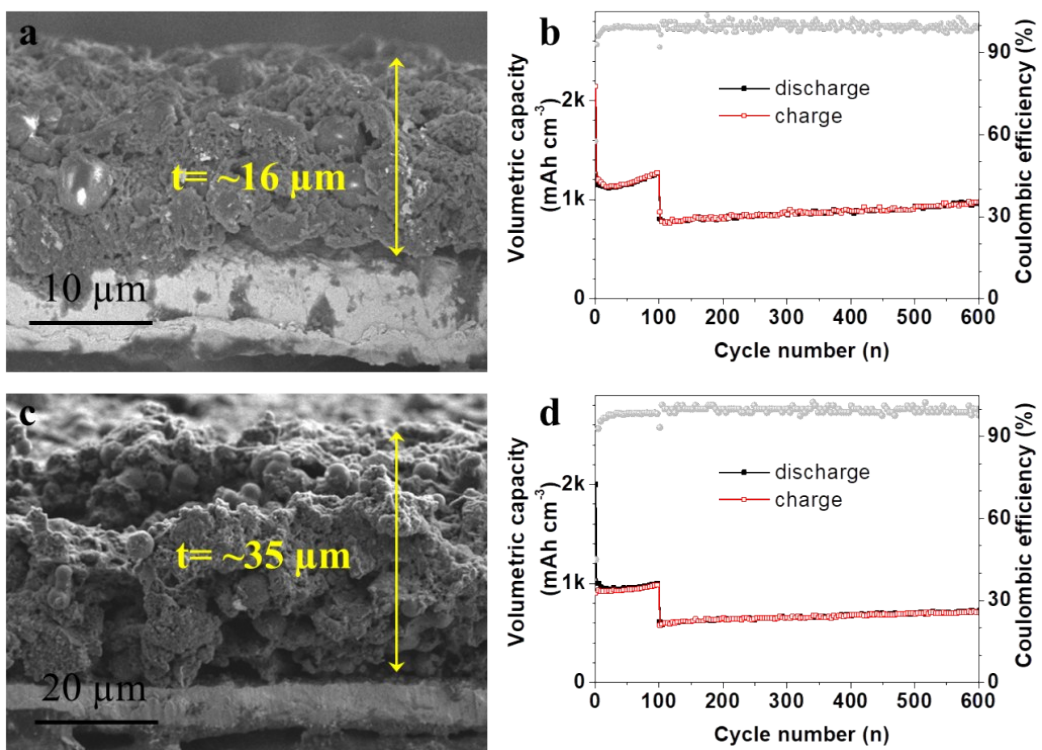


Figure S9. Long-life cycling and corresponding volumetric capacity of the electrode thickness from 16 to 35 μm at the current densities of 0.5 and 1.0 A g^{-1} for 100 and 500 cycles, respectively.

Table S1 Compositions of NCM, NC and C.

Samples	S_{BET} ($\text{m}^2 \text{g}^{-1}$) [a]	At.% [b]			N/C species (absolute/relative content)		
		C	N	O	N1	N2	N3
NCM	322.7	87.2	5.6	7.2	0.7 (11%)	2.5 (39%)	3.2 (50%)
NC	213.5	86.8	5.7	7.5	1.9 (29%)	3.1 (48%)	1.6 (23%)
C	94.6	89.3	N.A.	10.7	N.A.		

Note: N.A. not available. [a] S_{BET} is BET specific surface area. [c] Atomic concentrations from the XPS data. N1: pyridinic-N. N2: pyrrolic-N. N3: graphitic-N.

Table S2 ORR activities of NCM versus recent reported N-doped metal-free carbons.

Samples	Precursors of CDs	Synthesis methods	N (at.%)	Catalyst loading (mg cm ⁻²)	E _{onset} (V vs. RHE)	E _{1/2} (V vs. RHE)	Refs.
NCM	chitosan + gallic acid	Hydrothermal	5.6	0.12	0.996	0.818	This study
NMC	polypyrrole + phytic acid + polystyrene sphere	Polymerization + pyrolysis (900 °C)	3.56	0.20	N.A.	0.81	[1]
NCN-1000-5	citric acid + NH ₄ Cl	Pyrolysis + carbonization (1000 °C)	2.46	N.A.	0.95	0.82	[2]
N-doped microporous carbon	banana peel + melamine	Carbonization (400 °C) + pyrolysis (1000 °C)	3.0	0.10	-0.085	N.A.	[3]
NCYS	PPy	Pyrolysis (900 °C, Ar)	3.24	0.64	0.93	0.81	[4]
NS-MHCS	sodium 1,5-naphthalenedisulfonate + polydopamine + silica SBA-15	Hard template + carbonization (800 °C)	2.04	0.16	0.945	0.812	[5]
HNC	Aniline + K ₃ [Fe(CN) ₆]	Polymerization + carbonization (900 °C)	1.95	0.50	1.001	0.796	[6]
THNCM	glucose + dicyandiamide	Hydrothermal + carbonization (800 °C)	4.88	0.81	0.92	N.A.	[7]
NCMSs	<i>o</i> -methylaniline + H ₃ PO ₄ + H ₂ O ₂ + FeCl ₃	Hydrothermal + carbonization (900 °C)	1.86	0.20	0.981	0.815	[8]
N-CSH	porous silica microspheres + pyrrole + hydrofluoric acid	Template + carbonization (850 °C) + dissolve the framework	8.0-8.8 wt.%	0.10	0.927	N.A.	[9]
NGHMs	polystyrene microspheres + H ₂ SO ₄ + poly(ethyleneimine) + graphene oxide nanosheets + melamine	Sacrificial template+ pyrolysis (800 °C)	2.73	2.55	0.934	0.777	[10]
N-CB	carbon black	Two-step heating procedures (750 + 800 °C)	0.7	N.A.	0.97	0.82	[11]

Table S3 Volumetric capacities of other anode materials for LIBs.

Samples	Density (g cm ⁻³)	Refs.
NCM	1.55	This study
INCM	1.59	[12]
I-doped graphene	0.39	[13]
N-doped holey graphene	1.1	[14]
Modified hard carbon aerogel	~1.5	[15]
Sn(IV)@Ti ₃ C ₂	2.16	[16]
Si-C composites	0.49	[17]
Si/graphene/graphite foam	1.03	[18]
SnO ₂ @GC	2.18	[19]
Hollow structured SnO ₂ @Si nanospheres	1.33	[20]
CNC	2.06	[21]

References

- [1] Z. Zhang, J. Sun, M. Dou, J. Ji, F. Wang, Nitrogen and phosphorus codoped mesoporous carbon derived from polypyrrole as superior metal-free electrocatalyst toward the oxygen reduction reaction, *ACS Appl. Mater. Interfaces*, 9 (2017) 16236-16242.
- [2] H. Jiang, J. Gu, X. Zheng, M. Liu, X. Qiu, L. Wang, Z. Chen, X. Ji, J. Li, Defect-rich and ultrathin N doped carbon nanosheets as advanced trifunctional metal-free electrocatalysts for the ORR, OER and HER, *Energ. Environ. Sci.*, 12 (2019), 322-333.
- [3] L.-Y. Zhang, M.-R. Wang, Y.-Q. Lai, X.-Y. Li, Nitrogen-doped microporous carbon: An efficient oxygen reduction catalyst for Zn-air batteries, *J. Power Sources*, 359 (2017) 71-79.
- [4] Z. Jinqiu, W. Mengfan, Q. Tao, L. Sisi, C. Xuecheng, Y. Tingzhou, Y. Ruizhi, Y. Chenglin, Porous yolk–shell microspheres as N-doped carbon matrix for motivating the oxygen reduction activity of oxygen evolution oriented materials, *Nanotechnology*, 28 (2017) 365403.
- [5] H. Zhao, Y.-P. Zhu, L. Ge, Z.-Y. Yuan, Nitrogen and sulfur co-doped mesoporous hollow carbon microspheres for highly efficient oxygen reduction electrocatalysts, *Int. J. Hydrogen Energy*, 42 (2017) 19010-19018.
- [6] R. Wu, S. Chen, Y. Zhang, Y. Wang, W. Ding, L. Li, X. Qi, X. Shen, Z. Wei, Template-free synthesis of hollow nitrogen-doped carbon as efficient electrocatalysts for oxygen reduction reaction, *J. Power Sources*, 274 (2015) 645-650.
- [7] X. Liu, L. Li, W. Zhou, Y. Zhou, W. Niu, S. Chen, High-performance electrocatalysts for oxygen reduction based on nitrogen-doped porous carbon from hydrothermal treatment of glucose and dicyandiamide, *ChemElectroChem*, 2 (2015) 803-810.
- [8] Y. He, X. Han, Y. Du, B. Song, P. Xu, B. Zhang, Bifunctional nitrogen-doped microporous

carbon microspheres derived from poly(o-methylaniline) for oxygen reduction and supercapacitors, *ACS Appl. Mater. Interfaces*, 8 (2016) 3601-3608.

- [9] G.A. Ferrero, K. Preuss, A.B. Fuertes, M. Sevilla, M.M. Titirici, The influence of pore size distribution on the oxygen reduction reaction performance in nitrogen doped carbon microspheres, *J. Mater. Chem. A*, 4 (2016) 2581-2589.
- [10] W. Yan, L. Wang, C. Chen, D. Zhang, A.-J. Li, Z. Yao, L.-Y. Shi, Polystyrene microspheres-templated nitrogen-doped graphene hollow spheres as metal-free catalyst for oxygen reduction reaction, *Electrochim. Acta*, 188 (2016) 230-239.
- [11] J. Oh, S. Park, D. Jang, Y. Shin, D. Lim, S. Park, Metal-free N-doped carbon blacks as excellent electrocatalysts for oxygen reduction reactions, *Carbon*, 145 (2019), 481-487.
- [12] D. Wang, J. Zhou, J. Li, Y. Wang, L. Hou, F. Gao, Iodine and nitrogen-codoped carbon microspheres for ultrahigh volumetric capacity of Li-ion batteries, *ACS Sustain. Chem. Eng.*, 6 (2018) 7339-7345.
- [13] Y. Zhan, B. Zhang, L. Cao, X. Wu, Z. Lin, X. Yu, X. Zhang, D. Zeng, F. Xie, W. Zhang, J. Chen, H. Meng, Iodine doped graphene as anode material for lithium ion battery, *Carbon*, 94 (2015) 1-8.
- [14] X.P. Wang, L.X. Lv, Z.H. Cheng, J.A. Gao, L.Y. Dong, C.G. Hu, L.T. Qu, High-density monolith of N-doped holey graphene for ultrahigh volumetric capacity of Li-ion batteries, *Adv. Energy Mater.*, 6 (2016) 1502100.
- [15] Z.L. Yu, S. Xin, Y. You, L. Yu, Y. Lin, D.W. Xu, C. Qiao, Z.H. Huang, N. Yang, S.H. Yu, J.B. Goodenough, Ion-catalyzed synthesis of microporous hard carbon embedded with expanded nanographite for enhanced lithium/sodium storage, *J. Am. Chem. Soc.*, 138 (2016) 14915-14922.
- [16] J. Luo, X. Tao, J. Zhang, Y. Xia, H. Huang, L. Zhang, Y. Gan, C. Liang, W. Zhang, Sn⁴⁺ ion decorated highly conductive Ti₃C₂ mxene: Promising lithium-ion anodes with enhanced volumetric capacity and cyclic performance, *ACS Nano.*, 10 (2016) 2491-2499.
- [17] R. Yi, F. Dai, M.L. Gordin, S. Chen, D. Wang, Lithium - ion batteries: micro - sized si - c composite with interconnected nanoscale building blocks as high - performance anodes for practical application in lithium - ion batteries, *Adv.Energy Mater.*, 3 (2013) 273-273.
- [18] J. Ji, H. Ji, L.L. Zhang, X. Zhao, X. Bai, X. Fan, F. Zhang, R.S. Ruoff, Graphene-encapsulated Si on ultrathin-graphite foam as anode for high capacity lithium-ion batteries, *Adv. Mater.*, 25 (2013) 4673-4677.
- [19] J. Han, D. Kong, W. Lv, D.-M. Tang, D. Han, C. Zhang, D. Liu, Z. Xiao, X. Zhang, J. Xiao, X. He, F.-C. Hsia, C. Zhang, Y. Tao, D. Golberg, F. Kang, L. Zhi, Q.-H. Yang, Caging tin oxide in three-dimensional graphene networks for superior volumetric lithium storage, *Nat. Commun.*, 9 (2018) 402.
- [20] T. Ma, X. Yu, H. Li, W. Zhang, X. Cheng, W. Zhu, X. Qiu, High Volumetric Capacity of Hollow Structured SnO₂@Si Nanospheres for Lithium-Ion Batteries, *Nano Lett.*, 6 (2017) 3959-3964.
- [21] J. Jin, Z. Wang, R. Wang, J. Wang, Z. Huang, Y. Ma, H. Li, S. Wei, X. Huang, J. Yan, S. Li, W. Huang, Achieving High Volumetric Lithium Storage Capacity in Compact Carbon Materials with Controllable Nitrogen Doping. *Adv. Funct. Mater.*, 29 (2019), 1807441.